coatings

MDPI

Article

Influence of InGaZnO Films with Different Ratios on Refractive Index Sensing Characteristics of LPFG

Huanhuan Yan, Li Wang *, Shufeng Li, Huisong Zhang, Jin Wang and Peng Cheng

College of Physics and Optoelectronics, Faculty of Science, Beijing University of Technology, Beijing 100124, China; yhh1012528235@126.com (H.Y.); lishufeng@emails.bjut.edu.cn (S.L.); s201706110@emails.bjut.edu.cn (H.Z.); wangjin321@emails.bjut.edu.cn (J.W.); chengpeng@emails.bjut.edu.cn (P.C.)

* Correspondence: lwang.1@bjut.edu.cn

Received: 20 September 2020; Accepted: 13 October 2020; Published: 14 October 2020

Abstract: Sensitive materials are widely used in the field of optical fiber sensing because of their unique advantages such as rich types, controllable composition ratio and diverse structure distribution. In this paper, the surface of long-period fiber gratings with InGaZnO [(In_2O_3):(Ga_2O_3):(ZnO)] nano films with different compositions were coated by pulse laser deposition (PLD) technology. The best sensing ratio and the high sensitivity sensing of the refractive index of long-period fiber grating (LPFG) were achieved through the analysis of the influence of different ratios of InGaZnO nano films on the refractive index sensing characteristics of grating. High sensitivities of 337 nm/RIU (refractive index unit) and 145 dB/RIU of the LPFG are achieved when the best doping ratio of InGaZnO is 7:1:2.

Keywords: refractive index sensing; InGaZnO nanofilm; LPFG; PLD

1. Introduction

Due to the fast development of fiber drawing technology in the past 10 years, many high-performance and low-cost fiber components are available, which undoubtedly promotes the research and application of optical fibers in many fields such as sensing and detection [1–3]. Refractive index sensing is an important part of the optical fiber sensing field because the refractive index is the basic parameter of optical fiber detection. Other parameters can be detected directly or indirectly by detecting the change of refractive index [4]. Therefore, it is very important to expand the sensitive range of the refractive index and improve the detection sensitivity.

There are many kinds of common optical fiber-sensing component, such as fiber Bragg grating [5–7], tapered optical fiber [8,9], polished optical fiber [10] and etched optical fiber [11]. However, fiber Bragg grating is insensitive to refractive index. Other components damage the optical fiber too much, which makes the loss and leakage of transmitted light increase significantly. The detection part is very fragile, which is not conducive to practical application. In addition, it is difficult to control the size of a sensitive optical fiber accurately in the process of corrosion and polishing, which requires a high degree of technical requirements. However, the writing technology of long-period fiber grating (LPFG) is very mature and can precisely control the period and output wavelength [12,13].

Due to the limitations of optical fiber material, the optical fiber sensor can only detect the basic physical parameters such as temperature, stress, tension, and some parameters indirectly measured by these basic parameters. This greatly limits the scope of application of optical fibers and the further improvement of optical fiber-sensing sensitivity. In order to improve the sensitivity of optical fiber sensors and expand their application range, we propose the combination of material and optical fiber. At present, there are many kinds of sensing materials combined with optical fibers, including Cu, Au, Ag, graphene, ZnS, ZnO, etc. [14–16]. Most of the metal oxide films have characteristics of metal

conductivity and high optical transmittance. They have characteristic of high oxidation resistance and good stability. Therefore, they are favored by experts and scholars [17–19].

The ZnO film deposited at room temperature has a polycrystalline structure [20], and the presence of grain boundaries will deteriorate the overall performance of the film device. Therefore, In_2O_3 and Ga_2O_3 are introduced into the ZnO material, which act as network former to suppress the film crystallization. In the InGaZnO (IGZO) material system, $In3^+$ can form 5s electron orbits, which is very beneficial to the high-speed transmission of free carriers. The refractive index of the film can be adjusted by multi-element doping. As we know, different elements have unique physical and chemical properties. The multi-doping materials contain kinds of elements, so multi-doping materials often have special properties that a single material does not have. It is necessary and significant to study the influence of the multi-doping materials on the sensing characteristics of optical fiber.

There are many ways to coat nano-sensitive films, including magnetron sputtering, dip coating, drop coating, spin coating, vacuum evaporation, pulse laser deposition (PLD), etc. [21–23]. The PLD technology can not only prepare nano films in vacuum, but also change the ratio of target materials and the preparation parameters of nano films. The high-energy particles of PLD are beneficial to the epitaxial growth of thin films and the plasma transport produced by PLD technology makes the deposited films consistent with the target materials, so it is particularly suitable for the preparation of nano films with complex components and high melting-point materials.

In this paper, we use PLD technology to deposit IGZO nano films with different composition ratio on the surface of LPFG. By analyzing the optical and sensing properties of the prepared nano film, such as transmittance, refractive index and surface roughness, the best material ratio was found out and the high sensitivity was reached. IGZO is a multi-doping material with high electron mobility and flexible display, which will play an important role in promoting and referencing multi-parameter, flexible conductive materials and other multi-performance elements in future sensors.

2. Principles and Experimental Details

Principle

The four-layer model of the grating is used to analyze the transmission spectrum, the effective refractive index of the mode, as well as the coupling coefficient between the cladding mode and the core mode. The four-layer model contains core, cladding, film, and environmental layer. The resonant wavelength of LPFG is given as [24]:

$$\left(n_{eff_{01}^{co}} - n_{eff_{1,l}^{cl}}\right)\Lambda = \lambda_{res} \tag{1}$$

where λ_{res} is the resonance wavelength, $n_{eff_{01}^{co}}$ and $n_{eff_{1,i}^{cl}}$ are the effective refractive index of the fundamental core mode and cladding mode, Λ is the periodicity of grating.

The coupling between the core mode and the ith cladding mode of the grating can be presented as [25]:

$$T = \cos^2\left(K_{1i-11}^{cl-co}L\right) \tag{2}$$

where L is the length of grating. K_{1i-11}^{cl-co} is the coupling coefficient [26].

The nano thin film was coated on the surface LPFG. The four-layer model was used to analyze the influence of nano film on transmission characteristics of LPFG in theory [26]. In the experiment, IGZO nano films with different composition ratio were deposited by PLD. The influence of the ratio on the optical properties of the prepared nano films and the influence of the LPFG sensing characteristics were detected and analyzed under the condition of certain deposition time, laser power, vacuum degree, pressure and temperature. The best growth ratio of nano films were found through theoretical analysis and experimental detection, and a high-sensitivity refractive index sensor was prepared.

The effective refractive index of the cladding mode increases with the environmental refractive index when the refractive index of the film is constant as shown in Figure 1. As the mode increases, the refractive index changes significantly, thereby increasing the sensitivity. According to the phase-matching condition, with the increasing of the effective refractive index of the cladding, the resonance wavelength increases. As the effective refractive index of the film increases, the conversion interval shows a trend of first increasing and then decreasing. A second mode conversion will occur when the effective refractive index of the film increases to a certain extent, which reduced the first scope of the conversion interval. When the film refractive index is 1.68, the linear range of effective refractive index of the HE1,8 mode is the largest (1.43–1.45), which can be obtained from Figure 1a–d. We should adjust the doping ratio of the IGZO material so that the refractive index of the film is nearly 1.68.

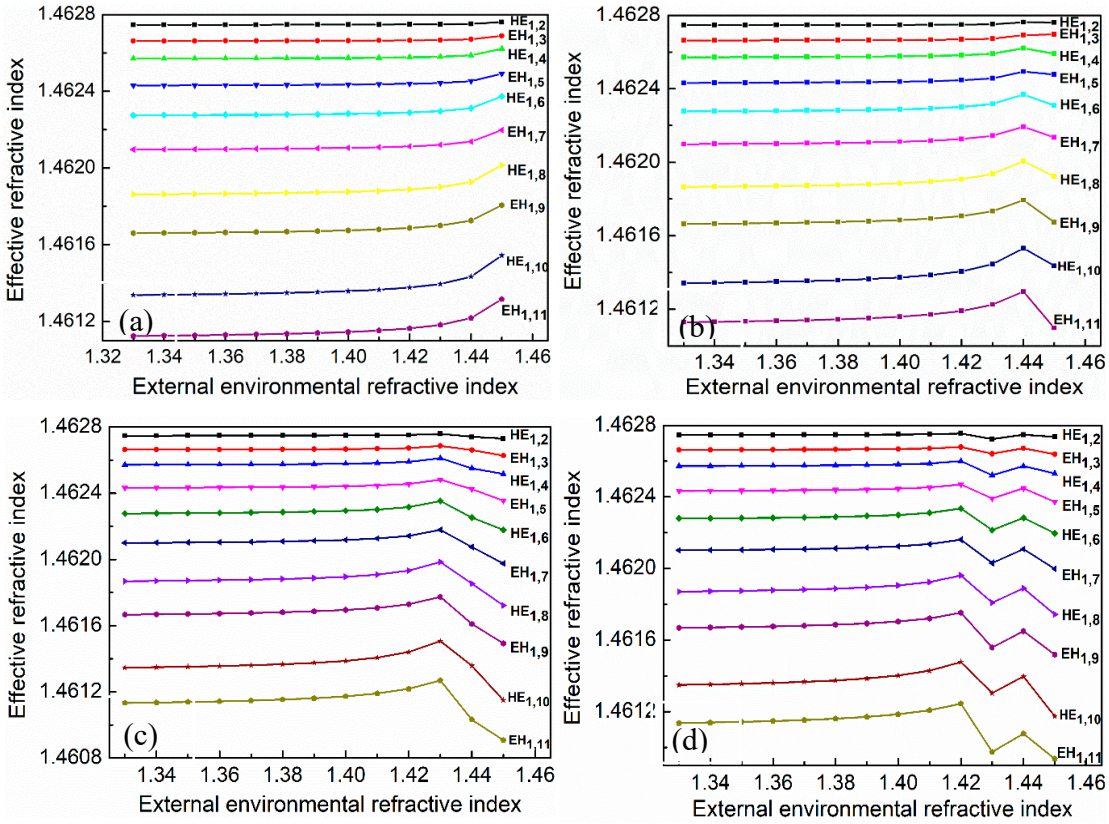

Figure 1. Effective refractive index of the first 10 cladding modes varies with the environmental refractive index, (**a**) $R_{InGaZnO}$ = 1.6, (**b**) $R_{InGaZnO}$ = 1.65, (**c**) $R_{InGaZnO}$ = 1.68, (**d**) $R_{InGaZnO}$ = 1.7.

The relationship between coupling coefficient and film refractive index of LPFG is simulated in Figure 2. The refractive index of the sensitive material is relatively high and stable when coupling a coefficient range of 1.45–1.68 and 2.1–2.5, which is suitable for sensing. The coupling coefficient can not only reflect the coupling ability but also affect the sensor sensitivity. The sensitivity increases with increasing coupling coefficient. The phase-matching condition shows that the greater the effective refractive index of the cladding, the higher the system sensitivity. Due to the limitations of coating methods, when the refractive index of the material is greater than 2.1, the material will crystallize, which will increase the surface roughness of the film and seriously affect the sensing performance. Therefore, we control the refractive index of the film material to around 1.68 which gives the same results in Figure 1.

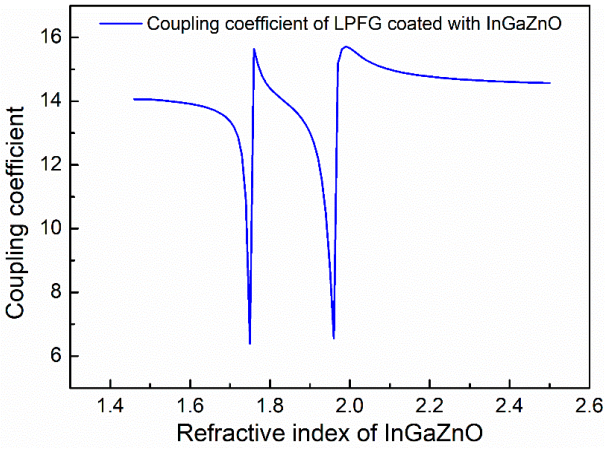

Figure 2. Relationship between coupling coefficient and film refractive index of long-period fiber grating (LPFG).

3. Materials and Methods

The coating process of LPFG is shown in Figure 3a. The first part is the selection process of grating (grating period and transmission intensity), the second part is grating cleaning, including deionized (DI) water cleaning and anhydrous ethanol cleaning, grating fixing and vacuuming, and the last part is the deposition of nano materials on the side of grating. Figure 3b is the structure of a vacuum cavity. Figure 3c is the four layer membrane structure of LPFG. For the purpose of the work, a commercial LPFG in standard SMF28 fiber (dcore = 8.2 μm, dclad = 125.0 μm, and NA = 0.12) with Λ = 360 μm and a length of 40.0 mm was selected. The IGZO ceramic target (Zhong Nuo Advanced Material, Beijing, China) with purity of 99.99%, diameter of 15 mm, thickness of 5 mm was attached to a target holder for structural durability and was ablated by a frequency-tripled 355 nm of Q-switch Nd:YAG laser (GCR-170, Spectra Physics, Mountain View, CA, USA) with a pulse duration of 10 ns, repetition rate of 10 Hz, and a pulse energy of 30 mJ in the fabrication. A LPFG with period of 377 μm and period number of 53 was selected and fixed in the optical fiber base in this experiment. The crystalline quality and mechanical properties of the IGZO are greatly affected by the surface cleanliness of an LPFG, so the LPFG was placed in deionized water and alcohol in turn and cleaned for 5 times by rubber head droppers. A thermocouple was press against the reverse side of the substrate holder for detecting the temperature. The distance between the target and the optical fiber scaffolds was 45 mm. At first, the chamber was evacuated to a base pressure of 2.5×10^{-4} Pa using a turbo molecular pump backed with a rotary pump. Then, Ar gas was introduced to the vacuum chamber as the protective gas and the pressure was kept at 7×10^{-4} Pa. During deposition, the LPFG and target holder were rotated in 90° direction to obtain uniformly thick films and reduce pitting on the target. Prior to deposition on each run, a shield was placed before the substrate and the pre-ablation for clearing surface of the target was carried out. After the thermal equilibrium between the LPFG and its holder being reached, the IGZO thin films begin to be deposited on the LPFG using PLD. In order to study the transmittance and sensing property of different deposition materials, we used different molar ratios for (In_2O_3):(Ga_2O_3):(ZnO) targets. The average laser power and deposition time of all targets are 300 mW, 15min. The molar ratios for (In_2O_3):(Ga_2O_3):(ZnO) were set of 6:1:3, 7:1:2, 7.5:1:1.5, respectively. All samples were prepared for LPFG with IGZO film at a substrate temperature of 25 °C and Ar flow rate of 0.9 sccm (standard cubic centimeter per minute). The transmission spectra of the thin films were examined using U-4100 spectrometer. The refractive index was measured via an ellipsometry analyzer (Ellitop C7512, Beijing, China). The IGZO film measured by ellipsometer is grown on glass substrate, which is coating simultaneously with LPFG. The thicknesses of the IGZO nano-films were measured at the fiber cross-section using a scanning electron microscope (SEM, JSM-6520, JEOL, Akishima, Japan).

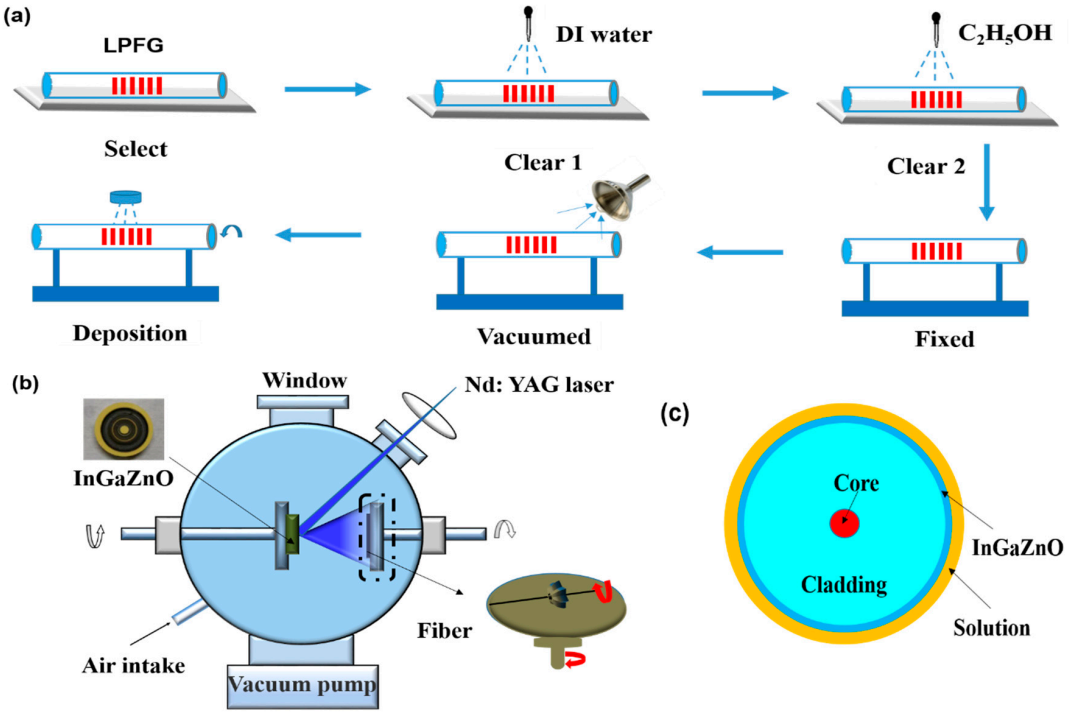

Figure 3. (**a**) Grating cleaning and coating process (**b**) Vacuum cavity structure (**c**) Four layer membrane structure of LPFG.

4. Results and Discussion

Figure 4 shows that the transmissivity of three groups of IGZO nano films with different ratios is relatively high, and the transmissivity is over 98% in the measured wavelength range. Three transmission spectra are highly coincident, which indicates that the change of indium oxide and zinc oxide composition has little effect on the transmittance of the nano film. The conditions of room temperature, 7 Pa and Ar are favorable for the growth of high transmittance nano sensitive films. Since the wavelength of optical fiber sensor is communication wavelength, we marked the transmissivity at 1550 nm.

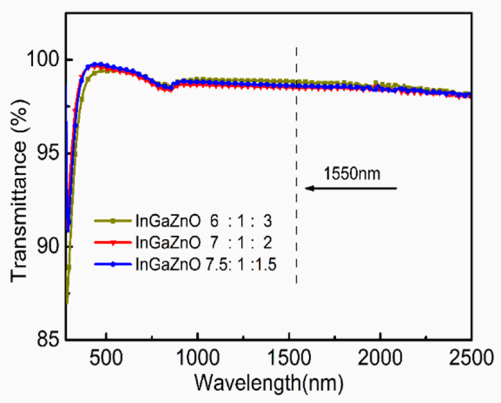

Figure 4. Transmission spectrum of nano film with different ratios.

The change of refractive index with wavelength of the prepared nano film measured by ellipsometry analyzer is shown in Figure 5. This shows that the refractive index of nano film decreases with the increase of wavelength. At the same wavelength, with the increase of the content of In_2O_3, the refractive index of the film increases first and then decreases. The atomic mass of Zn element is smaller than that of in element, so the prepared nano film increases with the increase of In_2O_3 content. However, with the increase of the content of In_2O_3, the grain size of the films increases further, resulting in the

increase of the gap and the decrease of the refractive index. According to the theory of the four-layers model, the higher the refractive index of the sensitive film, the higher the sensitivity to the external solution [27]. When the doping ratio is 7:1:2, the refractive index of the film at the wavelength of 1550 nm is 1.68.

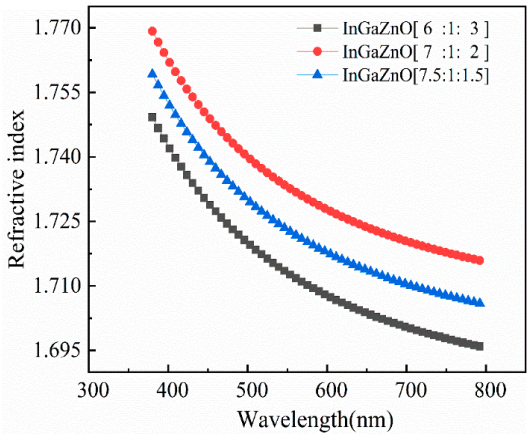

Figure 5. Relationship between refractive index of thin film.

In order to study the effect of different ratio of IGZO ceramic targets on the deposition of IGZO thin films, atomic force microscopy (AFM) was used to measure the samples to understand the surface morphology. Figure 6 shows the AFM image of IGZO nano film prepared at the ratio of 6:1:3, 7:1:2 and 7.5:1:1.5, respectively. Figure 6a shows that the surface particles of the film samples prepared at 6:1:3 are relatively small, uniform and orderly arranged, and the maximum peak value in the 1 × 1 μm measurement area is only 6.74 nm. With the increase of the ratio, the particles on the surface of the sample begin to appear relatively obvious coarse particles, as indicated in Figure 6c.

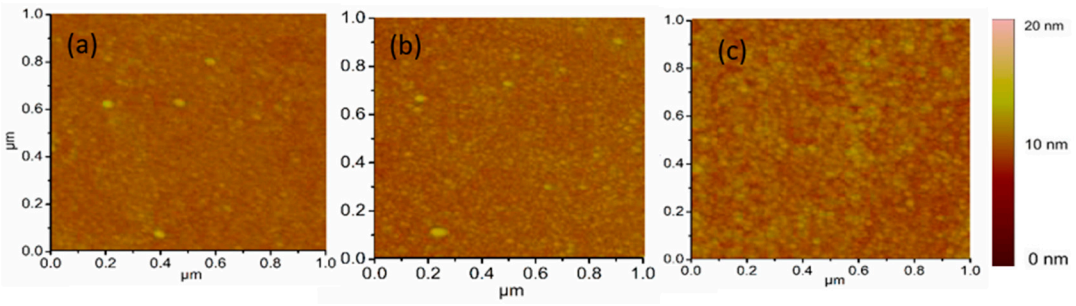

Figure 6. Atomic force microscopy (AFM) image of InGaZnO film at different content ratio, PA (In2O3):(Ga_2O_3):(ZnO) content is (**a**) 6:1:3, (**b**) 7:1:2, (**c**) 7.5:1:1.5.

Figure 7 shows the relationship between the surface roughness of the film and the content of In_2O_3. It can be seen that the root mean square roughness of the films increases with the increase of the content of In_2O_3. When the content of In_2O_3 is 60%, the root mean square roughness of the film reaches the minimum value of 0.492. When the content of In_2O_3 is 70% and 75%, the root mean square roughness is 0.591 and 0.793, respectively. When the content of In_2O_3 is 60%, 70% and 75%, the square arithmetic mean roughness is 0.37, 0.453 and 0.636 respectively. The percentage of surface difference is 0.392%, 0.632% and 0.831%, respectively. Because the atomic mass and radius of in are larger than that of ZnO, the roughness of the films increases with the increase of In_2O_3 content. This is consistent with the experimental results of the refractive index of the film in Figure 5.

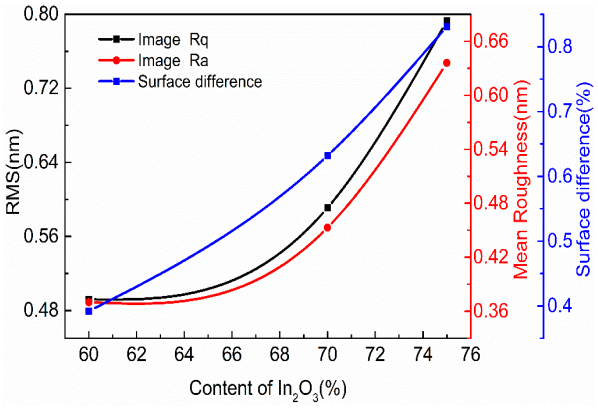

Figure 7. Change of square root mean roughness of InGaZnO film with the doping ratio of In_2O_3.

The X-ray diffraction (XRD) patterns of IGZO with different ratios are shown in Figure 8a. The broad spectrum shown in Figure 8a is consistent with the test result of Dr. Chen in our group [28]. The broad peak consists of 22° amorphous SiO_2 substrate peak and 32° IGZO peak. The wide peak near 32° can not be attributed to any specific phase of IGZO, which is the result of the contribution of different phases of IGZO materials. ZnO films grown at room temperature will be in crystalline state, and no crystallization peak of ZnO is observed in the film test results, which indicates that pure ZnO has been suppressed. Energy-dispersive X-ray (EDX) spectra of thin film with IGZO ratio of 7:1:2 is shown in Figure 8b. The material contains In, Ga, Zn and O elements are shown in Figure 8b. IGZO thin film is a combination of $InGaZn_4O_7$, $InGaZn_5O_8$, $InGaZn_2O_5$ and other materials [29]. At the same time, it is affected by oxygen and water molecules in the air, so that the element content is not completely consistent with the target ratio. X-ray photoelectron spectroscopy (XPS) spectra of thin films with IGZO ratio of 7:1:2 is shown in Figure 8c. The photoelectron peaks of C1s, In3d, O1s, Zn2p and Ga2p are shown in Figure 8c, which indicates that the film surface contains elements in, O, Zn and Ga. Element C may be caused by pollutants on the film surface, CO_2 gas or substance combustion during the detection process [30].

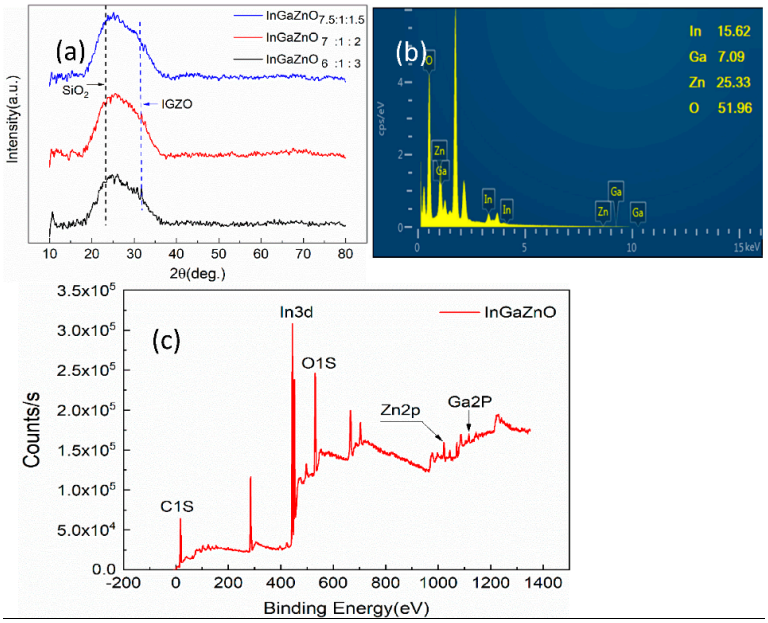

Figure 8. (**a**) X-ray diffraction (XRD) patterns of IGZO films, (**b**) energy-dispersive X-ray (EDX) image of IGZO film, (**c**) X-ray photoelectron spectroscopy (XPS) patterns of InGaZnO film.

Figure 9 is the scanning electron microscope (SEM) image of IGZO nano thin film. In the process of preparation, the laser power, deposition time, vacuum degree and pressure are all the same, only the content of In_2O_3 and ZnO is slightly changed. Through the SEM test, the thickness of IGZO film are the same under three different ratios, so we only show one of the pictures. The thickness of IGZO nano film is 103 nm.

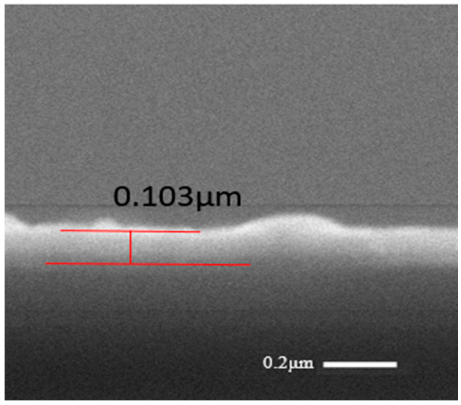

Figure 9. Scanning electron microscope (SEM) image of InGaZnO.

Figure 10 shows that the characteristic peak of LPFG moves towards the short wave direction with the increase of dissolved NaCl mass, which is blue shift and the transmission depth of the characteristic peak decreases accordingly. With the increase of NaCl mass, the refractive index of the solution increases and the effective refractive index of the cladding increases. We placed LPFG in different concentrations of NaCl solution, and calculated the refractive index of the solution by detecting the change of its transmission peak. At the same time, the sensing sensitivity of LPFG was also obtained. According to Equation (1), with the decrease of effective index difference between core and cladding, the peak of transmission wave moves to short wave. According to the principle of energy conservation, the shorter the wavelength, the stronger the energy. Therefore, the loss peak intensity decreases with the decrease of the wavelength. With the increase of In_2O_3 content in IGZO, the half peak width and transmission depth of LPFG become wider and narrower. Transmission depth and half peak width are two important parameters of grating performance [14]. With the increase of the refractive index of the detected solution, when the half width of the transmission peak of LPFG increases to twice of the original value and the transmission depth is half of the original value, we define it as the detection limit of LPFG. Beyond this limit, the stability and reliability of LPFG will be greatly reduced. Since Figure 10d has reached this limit, in order to ensure the stability of sensor detection, we do not increase the content of In_2O_3.

Figure 11a is a comparison diagram of the resonance wavelength of LPFG grating with the mass of dissolved NaCl. Figure 11b is a comparison diagram of the resonance intensity of LPFG grating with the mass of dissolved NaCl. The graphic symbol is the test data, and the line is the fitting line. Figure 11a shows that with the increase of dissolved NaCl mass, the peak wavelength moves to the short wave direction. The four fitting lines are highly consistent with the test data, so all four sensors can be used for the refractive index sensor test. The sensitivity of LPFG sensor is 42 nm/RIU. The wavelength sensitivity of the LPFG sensor is 272, 338, 327 nm/RIU when the ratio of IGZO is 6:1:3, 7:1:2 and 7.5:1:1.5. It is found that the wavelength sensitivity of the sensor after coating is 8 times of that before coating. Figure 11b shows that the peak strength decreases with the increase of dissolved NaCl mass. For precise detection, the optical fiber sensor has a high requirement for the stability of the sensor. The fitting straight line and the experimental data must be highly coincident. Therefore, only when the ratio of naked LPFG and IGZO is 7:1:2, the strength can be used as a parameter to detect the concentration of the solution. After coating the sensitive material, the strength of LPFG is affected by many factors, because the roughness of the film, the refractive index of the sensitive film, thickness

and other factors will affect the coupling efficiency of the grating and the film. The intensity sensitivity of the grating is 145 dB/RIU.

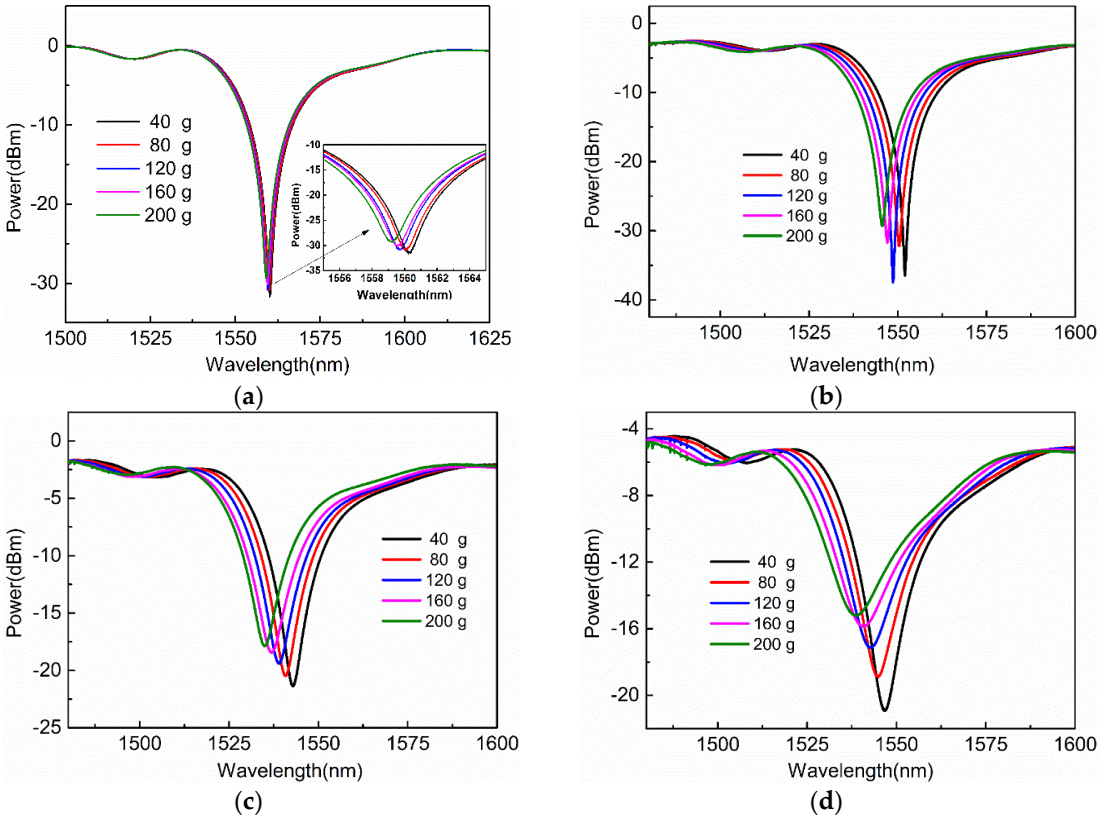

Figure 10. Transmission spectra of LPFG in different NaCl solutions, (**a**) uncoated LPFG, (**b**) LPFG coated with (In_2O_3):(Ga_2O_3):(ZnO) 6:1:3, (**c**) LPFG coated with (In_2O_3):(Ga_2O_3):(ZnO) 7:1:2, (**d**) LPFG coated with In_2O_3):(Ga_2O_3):(ZnO) 7.5:1:1.5.

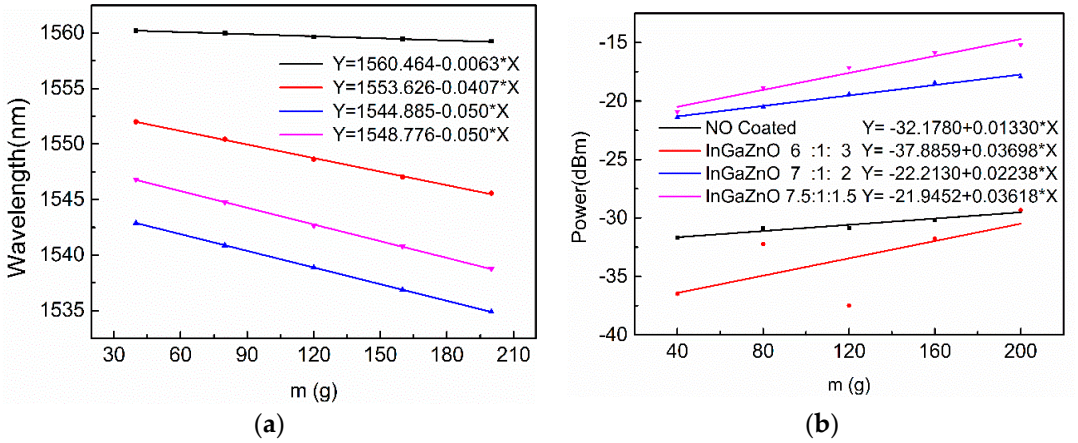

Figure 11. (**a**) Resonance wavelength of LPFG shifts with the mass of dissolved NaCl. (**b**) Resonance intensity of LPFG moves with the mass of dissolved NaCl.

5. Conclusions

According to the theoretical model of the four-layer mode, we have fabricated a four-layer LPFG grating sensor. We used PLD technology to coat IGZO nano thin films in different proportions, and analyzed the influence of material proportion on the nano films from the aspects of light transmittance, refractive index, surface morphology, roughness and so on. The sensing characteristics

of LPFG coated with IGZO and uncoated materials were compared. It was found that the sensitivity of LPFG coating material is greatly improved from 42 nm/RIU to 338 nm/RIU, which is about 8 times that before coating. When the ratio is 7:1:2, compared with other IGZO materials, the sensitivity of LPFG grating is the highest for 338 nm/RIU. In this ratio, the characteristic wavelength and intensity of LPFG grating change linearly with the solution concentration, and the stability and linearity are very high, that is to say, the wavelength and intensity can be used as the parameters of refractive index sensor detection. The fabricated sensor not only realizes the high sensitivity detection of the refractive index, but also provides conditions for multi-parameter detection. In addition, IGZO is a flexible conductive display material, and optical fiber has the characteristics of bending and anti-interference, which provides a new idea for seawater detection and real-time display.

Author Contributions: H.Y. and L.W. are contribute to design and discussion; Writing, H.Y.; Project administration, S.L. and H.Z.; Review and Editing, J.W. and P.C. All authors have read and agreed to the published version of the manuscript.

Funding: This work is funded by the National Natural Science Foundation of China under Youth Science Foundation Project (NSFC-61805005), The National Natural Science Foundation of China (NSFC-61473023).

Conflicts of Interest: The authors declare no conflict of interest.

References

1. Dominik, M.; Leśniewski, A.; Janczuk, M.; Niedziółka-Jönsson, J.; Hołdyński, M.; Wachnicki, Ł.; Godlewski, M.; Bock, W.J.; Śmietana, M. Titanium oxide thin films obtained with physical and chemical vapour deposition methods for optical biosensing purposes. *Biosens. Bioelectron.* **2017**, *93*, 102–109. [CrossRef]
2. Tien, C.-L.; Mao, T.-C.; Li, C.-Y. Lossy Mode Resonance Sensors Fabricated by RF Magnetron Sputtering GZO Thin Film and D-Shaped Fibers. *Coatings* **2020**, *10*, 29. [CrossRef]
3. Juan-Colás, J.; Johnson, S.; Krauss, T.F. Dual-Mode Electro-Optical Techniques for Biosensing Applications: A Review. *Sensors* **2017**, *17*, 2047. [CrossRef]
4. Brzozowska, E.; Śmietana, M.; Koba, M.; Górska, S.; Pawlik, K.; Gamian, A.; Bock, W.J. Recognition of bacterial lipopolysaccharide using bacteriophage-adhesin-coated long-period gratings. *Biosens. Bioelectron.* **2015**, *67*, 93–99. [CrossRef]
5. Shen, C.; Zhang, Y.; Zhou, W.; Albert, J. Au-coated tilted fiber Bragg grating twist sensor based on surface plasmon resonance. *Appl. Phys. Lett.* **2014**, *104*, 71106. [CrossRef]
6. Jiang, B.; Lu, X.; Gan, X.; Qi, M.; Wang, Y.; Han, L.; Mao, D.; Zhang, W.; Ren, Z.; Zhao, J. Graphene-coated tilted fiber-Bragg grating for enhanced sensing in low-refractive-index region. *Opt. Lett.* **2015**, *40*, 3994–3997. [CrossRef]
7. Shao, L.Y.; Shevchenko, Y.; Albert, J. Intrinsic temperature sensitivity of tilted fiber Bragg grating based surface plasmon resonance sensors. *Opt. Express* **2010**, *18*, 11464–11471. [CrossRef]
8. Socorro, A.B.; Del Villar, I.; Corres, J.M.; Arregui, F.J.; Matias, I.R. Spectral width reduction in lossy mode reson-ance-based sensors by means of tapered optical fibre structures. *Sens. Actuat. B* **2014**, *200*, 53–60. [CrossRef]
9. Zhou, J.; Tian, H.; Yang, D.; Liu, Q.; Huang, L.; Ji, Y. Refractive index sensing utilizing parallel tapered nano-slotted photonic crystal nano-beam cavities. *J. Opt. Soc. Am. B* **2014**, *31*, 1746–1752. [CrossRef]
10. Del Villar, I.; Zubiate, P.; Zamarreño, C.R.; Arregui, F.J.; Matias, I.R. Optimization in nanocoated D-shaped optical fiber sensors. *Opt. Express* **2017**, *25*, 10743. [CrossRef]
11. Śmietana, M.; Koba, M.; Mikulic, P.; Bock, W.J. Towards refractive index sensitivity of long-period gratings at level of tens of μm per refractive index unit: Fiber cladding etching and nano-coating deposition. *Opt. Express* **2016**, *24*, 11897. [CrossRef]
12. He, Y.-J.; Lo, Y.-L.; Huang, J.-F. Optical-fiber surface-plasmon-resonance sensor employing long-period fiber gratings in multiplexing. *J. Opt. Soc. Am. B* **2006**, *23*, 801. [CrossRef]
13. Qi, L.; Zhao, C.-L.; Yuan, J.; Ye, M.; Wang, J.; Zhang, Z.; Jin, S. Highly reflective long period fiber grating sensor and its application in refractive index sensing. *Sens. Actuators B Chem.* **2014**, *193*, 185–189. [CrossRef]
14. Hu, H.; Deng, Z.-Q.; Zhao, Y.; Li, J.; Wang, Q. Sensing Properties of Long Period Fiber Grating Coated by Silver Film. *IEEE Photonics Technol. Lett.* **2015**, *27*, 46–49. [CrossRef]

15. Coelho, L.; Viegas, D.; Santos, J.L.; De Almeida, J.M.M.M. Characterization of zinc oxide coated optical fiber long period gratings with improved refractive index sensing properties. *Sens. Actuators B Chem.* **2016**, *223*, 45–51. [CrossRef]
16. Hernaez, M.; Mayes, A.G.; Melendi-Espina, S. Graphene Oxide in Lossy Mode Resonance-Based Optical Fiber Sensors for Ethanol Detection. *Sensors* **2018**, *18*, 58. [CrossRef]
17. Wang, M.; Zhu, L.; Zhang, C.; Gai, G.; Ji, X.; Li, B.; Yao, Y. Lanthanum oxide @ antimony-doped tin oxide with high gas sensitivity and selectivity towards ethanol vapor. *Sens. Actuators B Chem.* **2016**, *224*, 478–484. [CrossRef]
18. Li, Z.H.; Shen, J.; Ji, Q.P.; Zhang, Y.J.; Ruan, X.K.; Dai, Y.; Cai, Z. Tuning the Resonance of the Excessively Tilted LPFG-Assisted Surface Plasmon Polaritons: Optimum Design Rules for Ultrasensitive Refractometric Sensor. *IEEE Photonics J.* **2018**, *10*, 1–14. [CrossRef]
19. Janczuk-Richter, M.; Piestrzyńska, M.; Burnat, D.; Sezemský, P.; Stranak, V.; Bock, W.J.; Bogdanowicz, R.; Niedziółka-Jönsson, J.; Smietana, M. Optical investigations of electrochemical processes using a long-period fiber grating functionalized by indium tin oxide. *Sens. Actuators B Chem.* **2019**, *279*, 223–229. [CrossRef]
20. Zhu, B.L.; Sun, X.H.; Zhao, X.Z.; Su, F.; Li, G.; Wu, X.; Wu, J.; Wu, R.; Liu, J. The effects of substrate temperature on the structure and properties of ZnO films prepared by pulsed laser deposition. *Vacuum* **2008**, *82*, 495–500. [CrossRef]
21. Ge, C.Q.; Xie, C.S.; Cai, S.Z. Preparation and gas-sensing properties of Ce-doped ZnO thin-film sensors by dip-coating. *Mater. Sci. Eng. B* **2007**, *137*, 53–58. [CrossRef]
22. Muthukrishnan, K.; Vanaraja, M.; Boomadevi, S.; Karn, S.R.K.; Singh, V.; Singh, P.K.; Pandiyan, K. Studies on acetone sensing characteristics of ZnO thin film prepared by sol–gel dip coating. *J. Alloy. Compd.* **2016**, *673*, 138–143. [CrossRef]
23. Nakagawa, Y.; Hara, K.O.; Suemasu, T.; Usami, N. On the Mechanism of $BaSi_2$ Thin Film Formation on Si Substrate by Vacuum Evaporation. *Procedia Eng.* **2016**, *141*, 23–26. [CrossRef]
24. Erdogan, T. Fiber grating spectra. *J. Lightwave Technol.* **1997**, *15*, 1277–1294. [CrossRef]
25. Tsao, C. *Optical Fiber Waveguide Analysis*; Oxford University Press: New York, NY, USA, 1992.
26. Erdogan, T. Cladding-mode resonances in short- and long-period fiber gratings filters. *J. Opt. Soc. Am. A* **1997**, *14*, 1760–1773. [CrossRef]
27. Wu, C.-H.; Jiang, G.-J.; Chang, K.-W.; Lin, C.-W.; Chen, K.-L. Highly sensitive amorphous In–Ga–Zn–O films for ppb-level ozone sensing: Effects of deposition temperature. *Sens. Actuators B Chem.* **2015**, *211*, 354–358. [CrossRef]
28. Chen, J.B.; Wang, L.Q.; Su, X.Q. Pulsed laser deposited InGaZnO thin film on silica glass. *J. Non-Cryst. Solids* **2012**, *358*, 2466–2469. [CrossRef]
29. Suresh, A.; Gollakota, P.; Wellenius, P.; Dhawan, A.; Muth, J.F. Transparent, high mobility InGaZnO thin films deposited by PLD. *Thin Solid Films* **2008**, *516*, 1326–1329. [CrossRef]
30. Swiatowska-Mrowiecka, J.; Maurice, V.; Zanna, S.; Klein, L.; Marcus, P.P. XPS study of Li ion intercalation in V_2O_5 thin films prepared by thermal oxidation of vanadium metal. *Electrochim. Acta* **2007**, *52*, 5644–5653. [CrossRef]